Cellulose (2021) 28:7877–7891
https://doi.org/10.1007/s10570-021-04026-y

ORIGINAL RESEARCH

Robust cellulose-carbon nanotube conductive fibers for electrical heating and humidity sensing

Jianhua Ma · Haihong Pu · Pengxin He · Qiangli Zhao · Shaoxue Pan · Yaowu Wang · Chen Wang

Received: 16 March 2021 / Accepted: 14 June 2021 / Published online: 22 June 2021

Abstract Multifunctional fibers have attracted widespread attention due to applications in flexible smart wearable devices. However, simultaneously obtaining a strong and functional woven fiber is still a great challenge owing to the conflict between the properties mentioned above. Herein, mechanically strong and highly conductive cellulose/carbon nanotube (CNT) composite fibers were spun using an aqueous alkaline/urea solution. The microstructure as well as physical properties of the resulting fibers were characterized via scanning electron microscopy, infrared spectroscopy, mechanical and electrical measurement. We demonstrated that carboxylic CNTs can be well dispersed in alkali/urea aqueous systems which also dissolved cellulose well. The subsequent wet spinning process aligned the CNTs and cellulose molecules inside the regenerated composite fiber well, enhancing the interaction between these two components and endowing the composite fiber having a 20% CNT loading with an excellent mechanical strength of 185 MPa. Benefiting from the formation of conductive paths, the composite fiber with the diameter of about 50 μm possessed an electrical conductivity value in the range of 64–1274 S/m for 5–20 wt% CNT loading. This excellent mechanical strength and high electrical conductivity enable the composite fiber to exhibit a great potential in joule heating; the heating temperature of cellulose/CNT-20 fiber reached more than 55 °C within 15 s at 9 V. In addition, the multifunctional filaments are further manufactured as a water sensor to measure humidity. This work provides a potential material that can be applied in the fields of wearable electronics and smart flexible fabrics.

Jianhua Ma and Haihong Pu have contributed equally.

J. Ma · H. Pu · P. He · Q. Zhao · C. Wang (✉)
School of Materials Science and Engineering, Xi'an Polytechnic University, Xi'an 710048, Shaanxi, China
e-mail: wangchen2231@xpu.edu.cn

J. Ma · C. Wang
Shaoxing Keqiao West-Tex Textile Industry Innovative Institute, Shaoxing (Keqiao) 312030, Zhejiang, China

S. Pan
State Key Laboratory of Molecular Engineering of Polymers, Fudan University, 2005 Songhu Road, Shanghai 200438, China

Y. Wang
Cooperative Innovational Center for Technical Textiles, Xi'an Polytechnic University, Xi'an 710048, Shaanxi, China

Graphic abstract

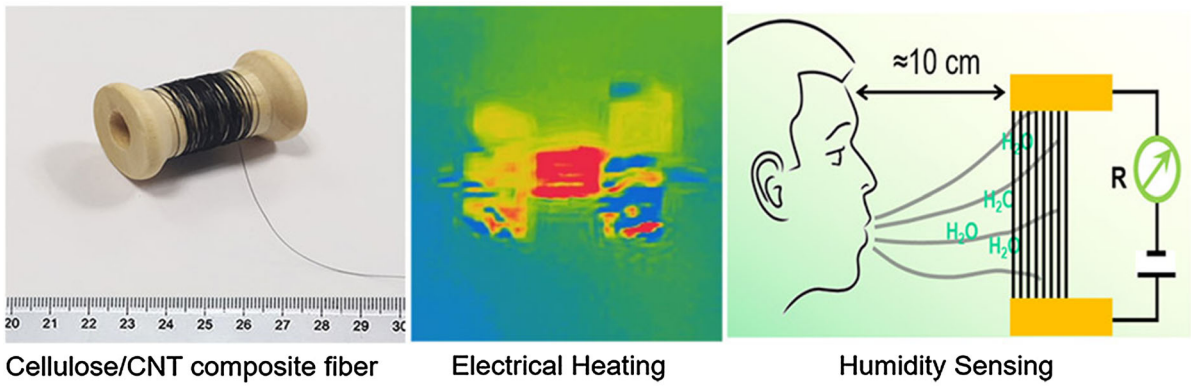

Keywords Cellulose fiber · Carbon nanotube · Electrical conductivity · Joule heating · Sensor

Introduction

Developing next-generation conductive, strong and tough eco-friendly fibers is urgent given their application potential in the areas of flexible smart wearable devices, such as sensors (Wan et al. 2019; Chen et al. 2018; Dichiara et al. 2017; Cho et al. 2019), electrical heaters (Zhao et al. 2020; Lee et al. 2016a, b) and electromagnetic interference (EMI) shielding fabric (Zhang et al. 2018; Lee et al. 2016a, b). Cellulose, as a typical natural fiber for garments, possesses biodegradability, chemical stability and skin-friendly properties compared with petroleum-based materials (Kontturi et al. 2018; Klemm et al. 2005). However, single cellulose fibers suffer from unbalanced mechanical performance (e.g., low toughness) and electrical insulating property, which significantly hinder its application in the latest functional fabric fields. To this end, considerable effort has been attempted to incorporate nanofillers into the cellulose matrix, including metal powders (Bober et al. 2014; Wang et al. 2017), carbon nanoparticles (Wan et al. 2019; Zhang et al. 2007; Hardelin and Hagstrom 2015) or conductive polymers (Shi et al. 2014), which endow the composite fiber with a certain electrical conductivity. Unfortunately, the aggregation of functional particles, as well as poor interfacial characteristics to the cellulose matrix, made it impossible to get adequate mechanical and electrical conductivity in the composite fiber at the same time. (Lee et al. 2016a, b; Hamedi et al. 2014; Huang et al. 2015).

Among the functional fillers, carbon nanotubes (CNTs) show a unique potential application value, as the long-range π-conjugation and large length: diameter ratio endow superior mechanical and electrical properties, making it valuable to prepare reinforced and conductive cellulose nanocomposites. Much work so far has focused on mixing CNTs with cellulose in a specific solution, such as ionic liquid (Zhang et al. 2007; Hardelin and Hagstrom 2015), N-methylmorpholin-N-oxide (NMMO) (Mahmoudian et al. 2017), or tetrabutylammonium acetate (TBAA)/dimethyl sulfoxide (DMSO) mixture solvent (Sun et al. 2015; Jiang et al. 2017a, b). Unfortunately, the solvent economy, environmental friendliness as well as the dispersion state of CNTs all will affect the preparation process of cellulose/CNT composite fibers. As an excellent water-soluble material, 2,2,6,6-tetramethylpiperidine-1-oxyl (TEMPO) oxidized cellulose nanofibrils were usually used to prepared cellulose/CNT composite films or fibers (Wan et al. 2019; Zhang et al. 2018; Koga et al. 2013). However, this material is hard to apply in the field of wearable textiles owing to its intrinsic water-solubility characteristic. Although there are reports that cellulose nanofibrils can act as a dispersion agent to assist CNT dispersal in aqueous solution, it is still hard to obtain a spinning dope with a high content of CNTs with excellent dispersion in cellulose solution (Carrasco et al. 2014; Ferreira et al.

2017). For instance, Zhang et al. (2007) reported a CNT-reinforced regenerated cellulose fiber via ionic liquid as the solvent, the resulting fiber containing 4 wt% CNTs exhibited excellent mechanical properties and a high electrical conductivity of 8.3×10^3 S/cm, whereas further increasing CNT content did not increase the electrical conductivity. Qi et al. (2015) studied CNT/cellulose composite fibers and demonstrated that the conductivity of the fiber increased with the CNT loading from 2 to 8 wt%, however, a slight decrease in both tensile strength and elongation at break is observed with CNT loading increase. In spite of efforts and resulting progress, simultaneously achieving strong, tough and conductive cellulose fiber is still an open issue.

In recent years, Zhang's team developed a series of novel green solvents, which include aqueous NaOH/urea (Cai et al. 2008; Jiang et al. 2014), NaOH/thiourea (Jiang et al. 2017a, b), and LiOH/urea solutions (Cai et al. 2007). When precooled to low temperature (between − 5 and − 12 °C), the cellulose can be dissolved rapidly to obtain a transparent cellulose solution. Owing to its low cost, recyclable, and environmentally benign features, this kind of solvent shows a good application prospect (Ye et al. 2019; Zhu et al. 2018; Qi et al. 2013). For CNTs, the hydrophilicity can be obtained through acid-treatment to introduce carboxyl functional groups (Wepasnick et al. 2011). Combining the water solubility characteristics of carboxylic CNT as well as the co-alkali system for cellulose dissolution, it is possible to prepare a composite fiber with high CNT filling. In the current study, to simultaneously realize conductivity, reinforcing and toughening cellulose-based nanocomposite fibers, we devised a convenient strategy including solution dispersion and wet spinning technology to produce cellulose/CNT filaments based on the NaOH/urea dissolving system. Carboxylic CNTs can not only disperse efficiently in alkaline aqueous solution, but also forms a tight bond with the hydroxyl group on the cellulose macromolecular surface. After the spinning dope is extruded through the limited space of the spinneret, the nanocellulose networks wrapping the CNTs formed a unidirectional arrangement and thus achieving a high-performance structural material. The composite fiber with the diameter of about 50 μm exhibited a high mechanical strength of 185 MPa and electrical conductivity value up to 1274 S/m for 20% CNT loading. Encouraged by this balanced performance, we further explored the application of joule heating and humidity sensing for the composite fiber. Such application expanded the potential value for these cellulose/CNT fibers in the smart wearable field.

Experimental section

Materials

Cellulose powder (particle diameter: 50 μm) was supplied from Aladdin Co., Ltd (Shanghai, China). Sodium hydroxide (NaOH), urea, concentrated sulfuric acid (H_2SO_4, 98%), nitric acid (HNO_3, 65%) and sodium sulfate (Na_2SO_4) were purchased from Sinopharm Chemical Reagent Co., Ltd. (Shanghai, China). Multiwalled carbon nanotubes (MWCNTs, diameter ranging 10–20 nm) were purchased from Nanjing XFNANO Materials Tech Co., Ltd, China. All the chemicals were in analytical grade and used without further purification.

Preparation of cellulose/cnt composite fibers

Carboxylic CNTs were synthesized by mixed acid treatment according to previous reports (Wepasnick et al. 2011; Blanchard et al. 2007). Typically, 1 g pristine MWCNTs and 80 mL mixed acid (H_2SO_4/HNO_3 = 3:1 in volume) were added into a round-bottom flask and dispersed in an ultrasonic bath for 30 min. Then the flask equipped with reflux condenser and magnetic stirrer was transferred to a water bath of 70 °C for 8 h. After reaction, the carboxylic CNTs were obtained after being washed by de-ionized water to neutral and freeze-dried.

A certain amount of carboxylic CNTs (0.25 g, 0.5 g, 0.75 g and 1 g) were well dispersed in 100 ml aqueous solution with 7 wt% NaOH/12 wt% urea via high-speed shear (20,000 rpm) mixing at room temperature. After that the mixed solution was precooled to − 12 °C, and 5 g cellulose powder was added to the precooled mixture with high-speed shear mixing at 0 °C for 2 h to obtain a homogeneous cellulose/CNT composite solution. The samples with the weight ratio of CNTs to cellulose was 5:100, 10:100, 15:100 and 20:100, which were denoted as C/CNT-5%, C/CNT-10%, C/CNT-15% and C/CNT-20%, respectively. For comparison, pure cellulose solution was also

fabricated under the same conditions and coded as Cellulose.

Set-spinning process was performed at room temperature on a modified wet-spinning set-up. The spinning dope was loaded into the syringe and then extruded through a syringe needle (diameter, 160 μm) into a coagulation bath of 10 wt % H_2SO_4/15 wt % sodium sulfate aqueous solution at 5 °C. The flow rate of the spinning dope through the syringe needle was 7 m/min. Then, the gel-state fibers were washed to remove the residual salts and acids, dried at room temperature until the weight stays the same, and finally obtained the cellulose/CNT composite fiber.

Characterization

The morphology of the prepared fibers was characterized by a field emission scanning electron microscope (FESEM) (Quanta-450) operating at an accelerating voltage of 10 kV, as the samples for the SEM investigations were treated by spray-gold. Rheological characterization of the spinning dope was conducted with a rotary rheometer (MCR302, Anton Paar). A shear rate sweep was performed at 25 °C from 10^{-1} to 10^3 s^{-1} to measure their apparent viscosity. A stress sweep was performed at 25 °C from 10^{-1} to 10^3 Pa with a constant frequency of 1 Hz. FTIR spectra of the composite fabric was obtained with a Spotlight 400 spectrometer in ambient condition. An average 32 scans with a resolution of 4 cm^{-1} in the range of wavelength 650–4000 cm^{-1} was employed in attenuated total reflectance (ATR) mode. Raman spectra were recorded using a Raman spectroscope (XploRA, HORIBA) with a 532 nm laser. Contact angle was measured on an OCA-20 contact angle system (Dataphysics, Germany) by dropping water (4 μL) onto the samples at ambient temperature. Average contact angles were obtained by measuring the same sample at five different positions. Thermogravimetric analysis (TGA, TA Instruments) was performed from 50 to 800 °C at a heating rate of 10 °C/min under air atmosphere. The mechanical and electrical properties of the fibers were measured with a universal testing machine (RWT-10, Reger) and a digital multi-meter (OWON B35T). The temperature change and thermal imaging feature of fabric were measured via an infrared thermal camera (FLIR ONE Pro).

Results and discussion

Preparation process of conductive cellulose/CNT fiber

To construct a CNT reinforced cellulose fiber, we firstly prepared the composite spinning dope followed by the implementation of the wet spinning process. Here we employed the precooled 7 wt% NaOH/12 wt% urea aqueous solution (− 12 °C) as the co-solvent to disperse the carboxylic CNT and dissolve microcrystalline cellulose, as the schematic diagram shown in Fig. 1a. Here, carboxylic CNT can be well dispersed in NaOH/urea aqueous solution, as there is no stratification or precipitation occur over a long time for the mixture. When solid cellulose is immersed into the precooled NaOH/urea solvent, NaOH hydrate interacts with hydroxyl groups on cellulose macromolecules will break the intra- and intermolecular hydrogen bonds of cellulose. Meanwhile, the dissolved cellulose can form a wormlike inclusion complex with urea as the shell packaged cellulose-NaOH hydrogen-bonded ligand in the alkaline aqueous solution (Cai et al. 2007). Based on the characteristic of co-solvents between carboxylic CNT and cellulose dissolution, a stable and uniform cellulose/CNT composite spinning dope can be acquired via high-speed mixing (Fig. 1a). Next, this spinning dope was extruded into a coagulation bath of H_2SO_4/$NaSO_4$, where solvent exchange and neutralization reaction were performed to form a stable gel fiber (Fig. 1b, c). The gel-state fiber was then dried under tension at room temperature and finally wound onto a spool for later use (Fig. 1d). Thanks to the good dispersion and tight bonding of carbon nanotubes in cellulose solution, the composite fiber with 20 wt% CNT still exhibited excellent flexibility, as this composite fiber can be knotted easily (Fig. 1e). Moreover, the efficiently filling of conductive material lead the composite fiber with outstanding conductivity, as shown in Fig. 1f that an LED can be lighted when using the composite fiber as a conductor under only 3 V.

Properties and characterization of the spinning dope

To obtain cellulose/CNT fibers through the wet spinning process, firstly the spinning dope should

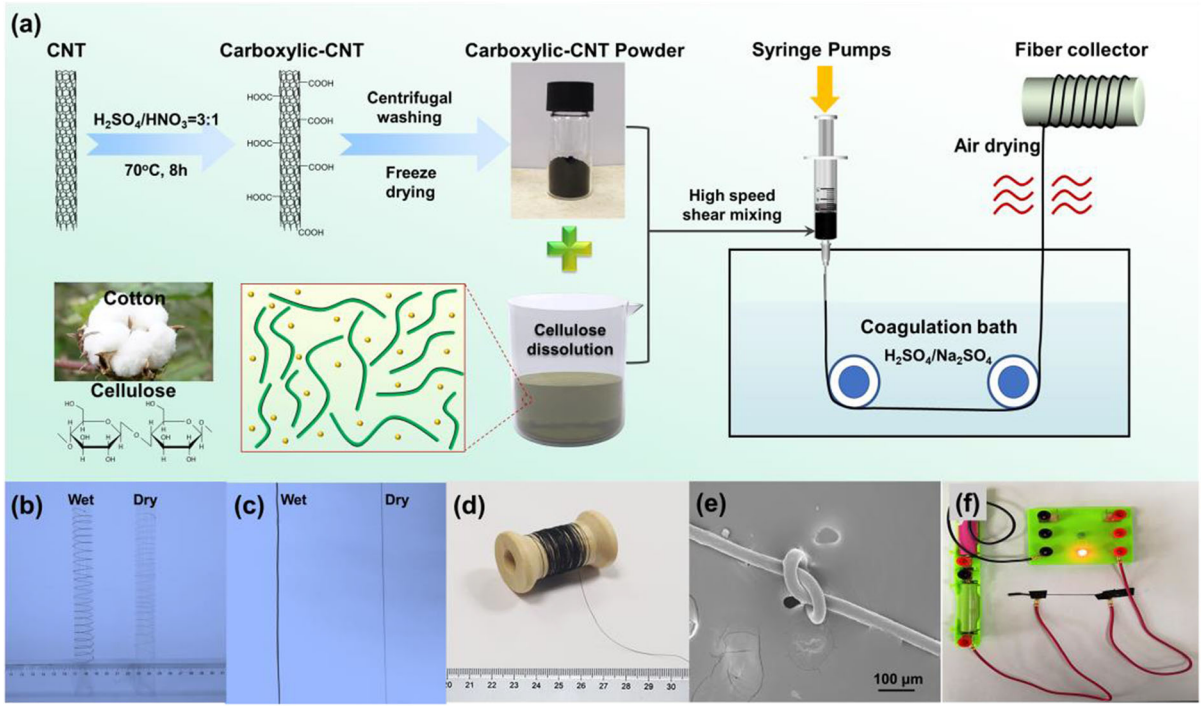

Fig. 1 **a** Schematic diagram for the preparation process of cellulose/CNT spinning solution as well as wet spinning process of cellulose/CNT composite fiber; **b**, **c** Digital image of the cellulose/CNT composite fiber with wet and dry state; **d** Digital image of dry cellulose/CNT composite fiber wound around a spool; **e** SEM image of knotted C/CNT-20% composite fiber filament; **f** C/CNT-20% composite fiber as a conductive line to light an LED

possess a proper rheological property for smooth extrusion. Here the diameter and length of the syringe needle was 160 μm and 12.7 mm (Fig. 2d), as this high aspect ratio (≈80) of the needle guarantees the effective alignment for cellulose molecules and CNTs during extrusion. Figure 2a shows the curves of viscosity as a function of shear rate for pure cellulose and CNT mixture. We can see that all samples displayed a shear-thinning behavior, which is vital for extrusion process. Figure 2b presents the corresponding storage modulus (G′) and loss modulus (G″) as a function of the shear stress. For cellulose and C/CNT-10% solution, G″ is always higher than G′ which means the solution maintains the property of viscous fluid state under test condition (Li et al. 2017; Siqueira et al. 2017), while an elastic viscous crossover located around 200 Pa appears for the C/CNT-20% sample, which indicate that the solution of C/CNT-20% can flow smoothly through the nozzle and partially preserve shape integrity after leaving the nozzle (Ma et al. 2019). This rheological characteristic also can be seen from the flowing state for the spinning dope, as shown in Fig. 2c. When the freely distributed CNTs enter the restricted space of the injection nozzle, this ultra-large aspect ratio material will be aligned with the flow direction of spinning solution. Meanwhile this oriented structure for CNTs can be effectively maintained to the composite fiber through the instant filament formation process in the coagulation bath. Benefiting from the shear thinning characteristics as well as the maintenance of the aligned structure for CNTs, we can always obtain a flexible composite fiber via solvent exchange in the coagulation bath, no matter whether for gel or liquid spinning dope.

Microstructure and properties characterization of the composite fiber

The successful implementation of the above strategy embeds CNTs into the cellulose network with favorable orientation, effectively enhancing the interaction between CNTs and cellulose fibrils. SEM images of both surface and cross section of cellulose composite fiber were shown in Fig. 3. The pristine cellulose fiber

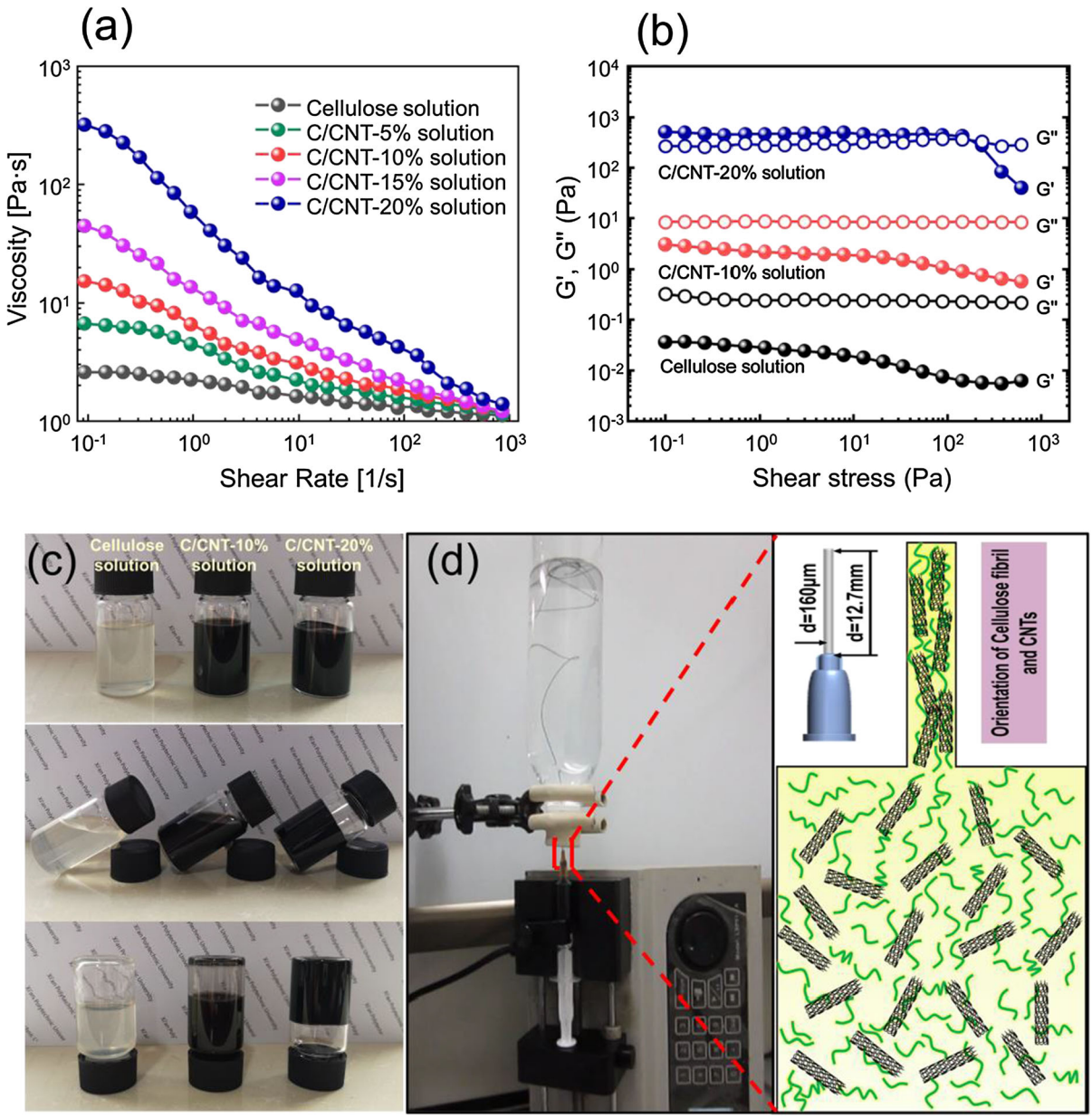

Fig. 2 **a** Viscosity versus shear rate curves of cellulose and C/CNT composite spinning dope; **b** Storage modulus (G′) and loss modulus (G″) versus shear stress curves of cellulose and C/CNT composite spinning dope; **c** Digital image of the cellulose spinning solution, C/CNT-10% and C/CNT-20% composite spinning dope; **d** Digital images of the wet spinning apparatus assembled in laboratory as well as the schematic diagram for the state of cellulose molecules and CNTs during extrusion

shows a smooth surface without visible grooves (Fig. 3a). After CNTs were added, significant grooves along the radial direction of the filament appeared on the surface of the composite fiber (Fig. 3c, d), which demonstrated that the CNTs embedded into cellulose network with favorable orientation. The cross section of the filament is almost a circle, no matter for cellulose or C/CNT composite fibers. For the investigated composite filaments, their diameters are always kept to about 50–60 μm which was attributed to the dense structure formed between CNTs and the cellulose matrix. Benefiting from this oriented

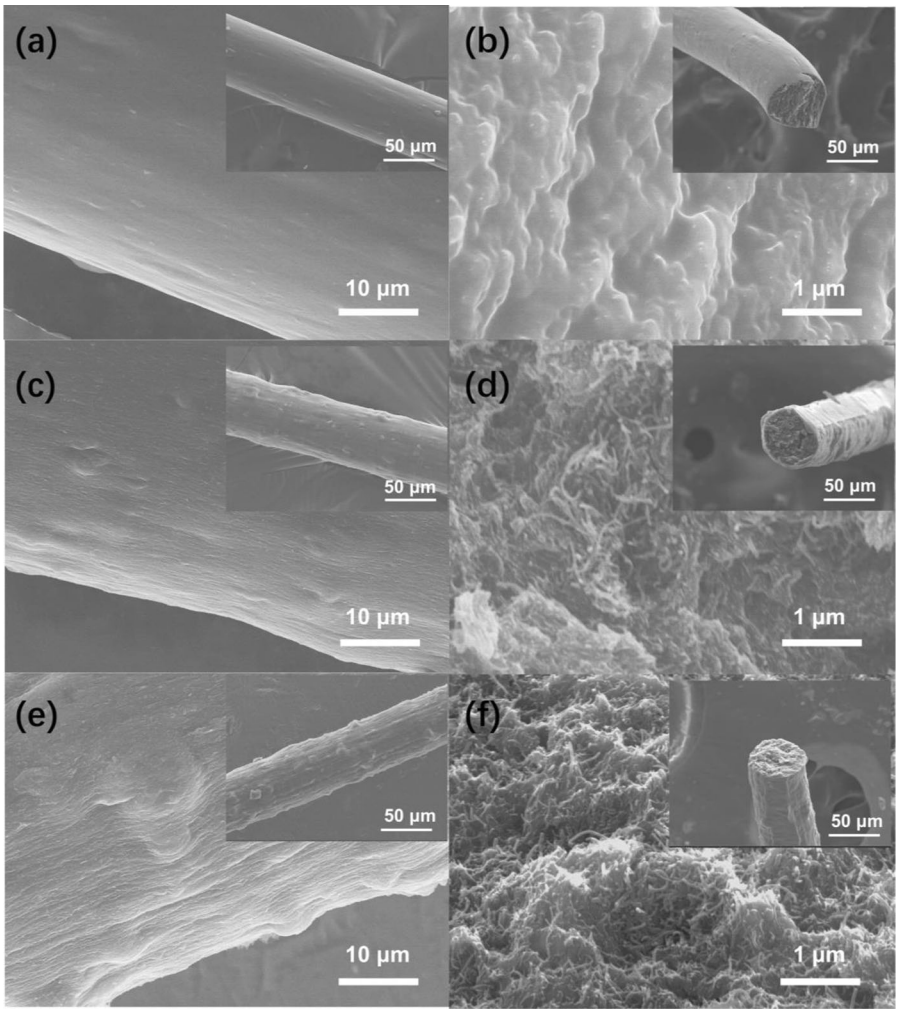

Fig. 3 **a**, **b** SEM images for the surface (**a**) and cross section (**b**) of pure cellulose fiber; **c**, **d** SEM images for the surface (**c**) and cross section (**d**) of cellulose/CNT-10% composite fiber; **e**, **f** SEM images for the surface (**e**) and cross section (**f**) of cellulose/CNT-20% composite fiber

arrangement as well as dense embedding structure, the composite fiber exhibited excellent physical and chemical properties, as can be seen in the following investigation.

The reason for this oriented arrangement as well as dense embedding structure of C/CNT fiber is attributed to the adequate interfacial interactions between CNTs and the cellulose matrix, which originated from hydrogen bonding, as deduction can be further demonstrated by Raman spectra and FTIR measurements. The Raman spectra of cellulose, C/CNT composite fibers as well as carboxylic CNTs are shown in Fig. 4a.Two characteristic peaks (I_D and I_G) of CNTs, 1337 and 1577 cm^{-1}, are attributed to disorder induced by defects in the nanotube lattice and in-plane vibration of the C−C bonds, respectively. No significant change of these two peaks was found for composite fibers compared to those of CNTs, which indicated that there is no obvious destruction of CNTs during the dissolution-regeneration process (Qi et al. 2015). As shown in Fig. 4b, the stretching vibration band of hydroxyl groups at around 3352 cm^{-1} in the pure cellulose fiber, substantially shifts to a lower wavenumber (3260 cm^{-1}) for the C/CNT-20% sample. This result can be ascribed to the hydrogen bonding between the residual hydroxyls on the CNT surfaces and the hydroxyl groups in the cellulose chains (Huang et al. 2015; Yan et al. 2008). TGA was

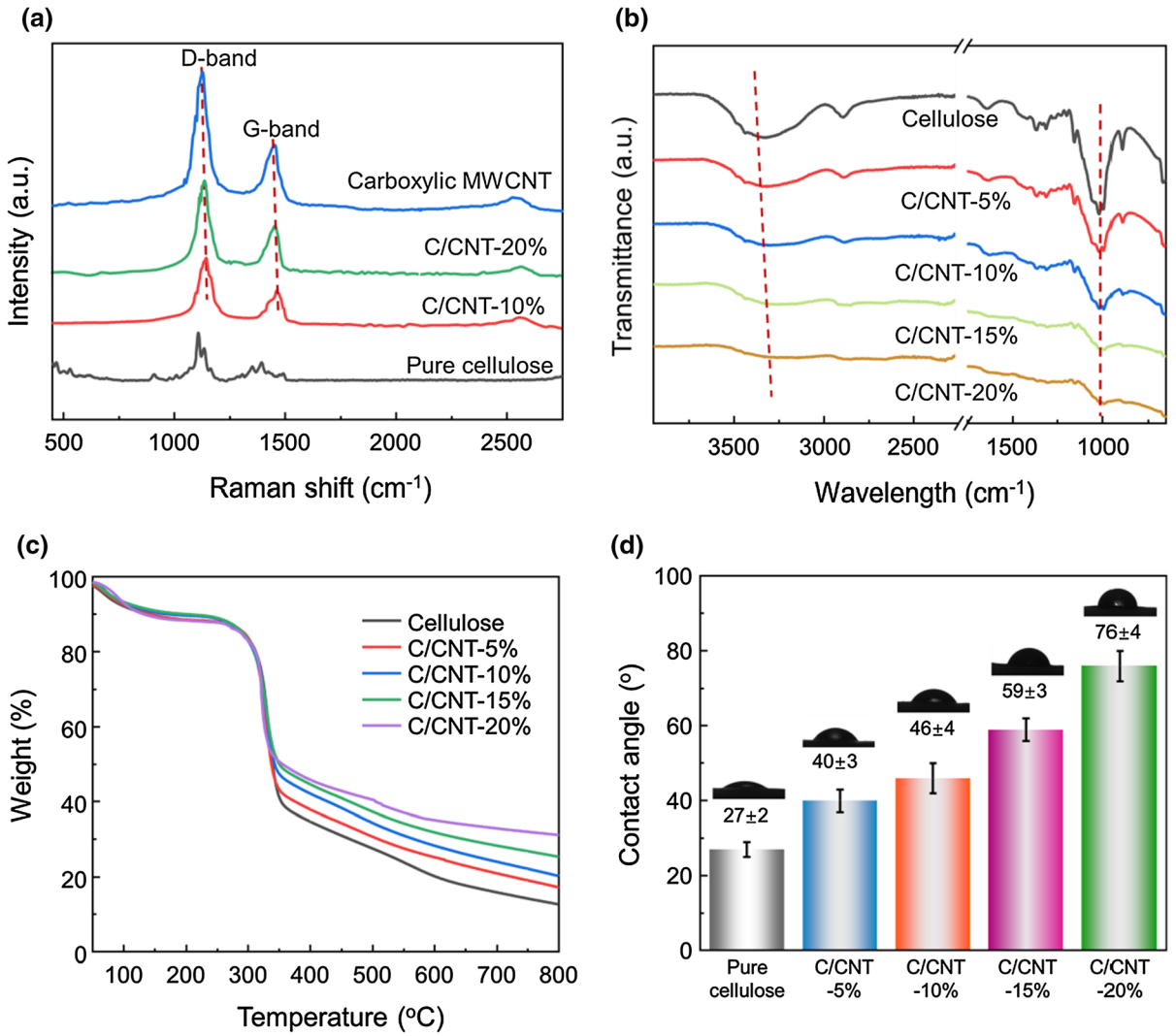

Fig. 4 **a** Raman spectra of regenerated cellulose and C/CNT composite fiber; **b** FTIR spectra of regenerated cellulose and C/CNT composite fiber. For clarity, a featureless region is omitted in the range of 2250–1750 cm^{-1}; **c** TGA curves of regenerated cellulose and C/CNT nanocomposite fiber. **d** Contact angle with water of regenerated cellulose and C/CNT composite fiber

carried out to verify the component proportions of the fiber (Fig. 4c); the weight loss around 100 °C mainly originated from elimination of the water molecules of the composite fiber. Meanwhile, the residual weight percentage of composite fiber kept a good agreement with the filling amount of CNTs, which indicated that the CNTs will not be lost during the solidification process. Contact angle was employed to elucidate the relationship between water molecules and C/CNT composite fiber. Figure 4d shows that the contact angle between water and tested filaments increases from 27 ± 2 to 76 ± 4° when the content of CNT varies from 0 to 20 wt%.

Typical stress–strain curves of cellulose and CNT filled composite fibers are shown in Fig. 5a. Notably, all the fibers fracture in a brittle manner with limited elongation at break and no distinct yielding, which should be attributed to the rigid nature of cellulose and CNTs. Compared with cellulose, adding carbon nanotubes will significantly enhance the mechanical properties of composite fiber. As shown in Fig. 5c, the cellulose fiber exhibited minimum tensile strength and Young's modulus, i.e., 114 ± 5 MPa and

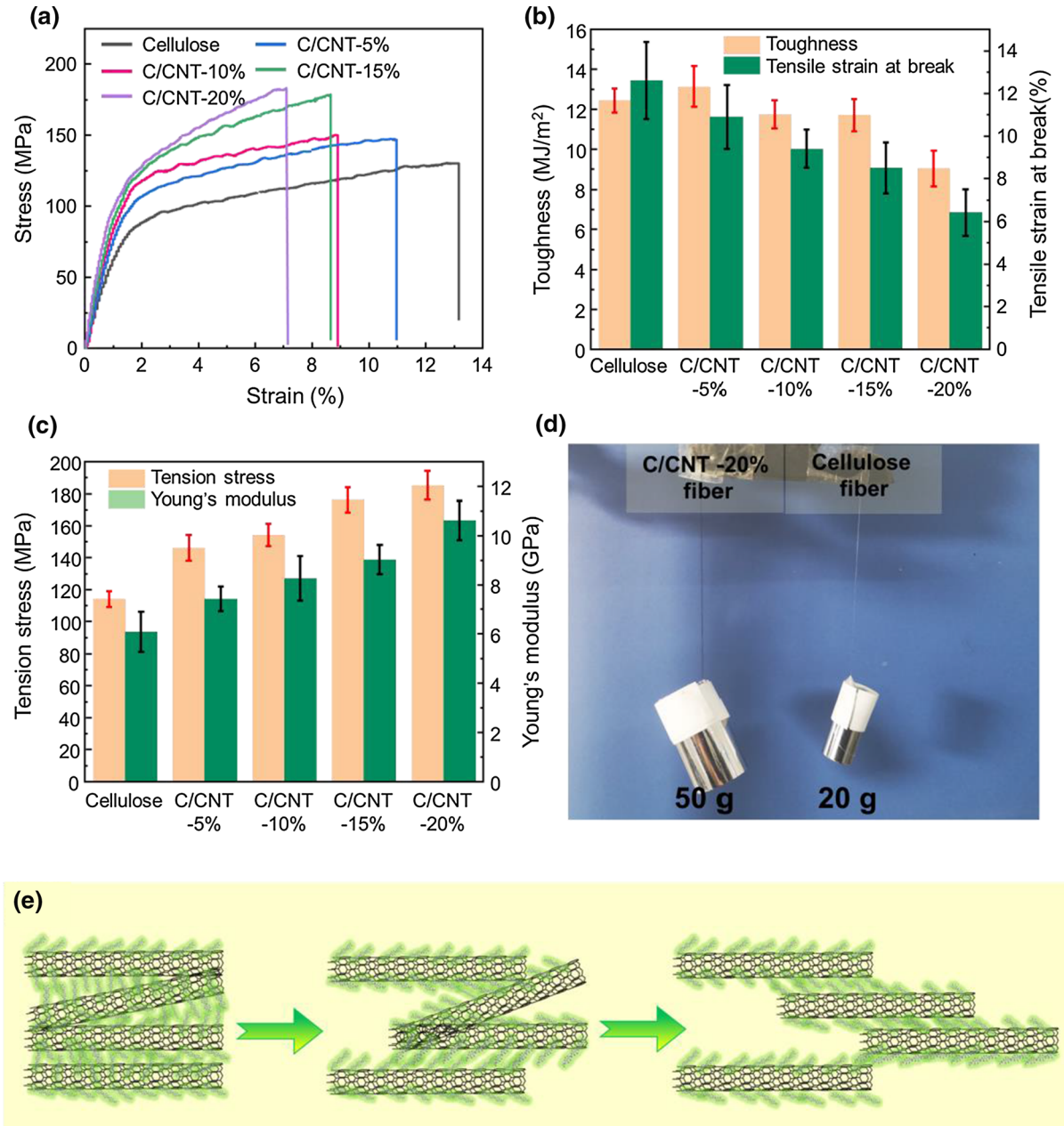

Fig. 5 **a** Stress–strain curves for regenerated cellulose fiber and C/CNT composite fiber; **b** Comparation of the toughness and elongation at break of regenerated cellulose fiber and C/CNT composite fiber; **c** Comparison of the Young's modulus and tension strength of regenerated cellulose fiber and C/CNT composite fiber; **d** Optical image of a weight weighing 50 g suspended by a 45 μm C/CNT-20% fiber as well as a weight weighing 20 g suspended by a 35 μm regenerated cellulose fiber; **e** Schematic to show the fracture process of the CNT reinforced cellulose fiber under tension

6.1 ± 1 GPa, respectively. When the CNT concentration rises to 20 wt%, the tensile strength and Young's modulus values reached to 185 ± 9 MPa and 10.6 ± 1 GPa, respectively, corresponding to the increases of 62% and 73% relative to the pure cellulose fiber. Here, C/CNT-20 fiber with a diameter of about 45 μm can withstand a weight of 50 g, whereas only 20 g for cellulose fiber with the diameter

of 35 μm (Fig. 5d). This phenomenon can be ascribed to the strong interfacial hydrogen bonding between cellulose and carboxylic CNTs, which has been demonstrated by FTIR results (Fig. 4b). Figure 5e illustrates that the hydrogen bonds as well as slip and release between the aligned CNTs will affect the stress transfer of the composite fiber. This eventually led to a greatly improved of the mechanical strength and Young's modulus of these C/CNT fibers. However, owing to the restrictive effect of CNTs on the movement of the cellulose molecules, it also leads to a decrease in the elongation at break of the composite fiber which can be seen in Fig. 5b.

Joule heating and moisture sensing application of C/CNT composite fiber

Owing to the formation of a conductive path via CNTs embedded (Fig. 6a), the composite fiber possessed an electrical conductivity value in the range of 64–1274 S/m for 5–20 wt% CNT loading (Fig. 6b). According to the Joule heating principle, the conductive fiber can be used as a potential wearable heater (Wang et al. 2019). An electric heating experiment with the C/CNT-20% fiber sample was carried out by monitoring temperature changes at constant applied voltages of 3 V, 6 V and 9 V, as can be seen in Fig. 6c. It can be seen that the steady-state maximum temperatures were increased with the applied voltage increasing (Lee et al. 2016a, b). For the test sample, the temperature increased rapidly when a certain voltage of 9 V was applied at 10 s, reached a maximum value within 20 s, and decreased quickly to room temperature when the applied voltage was off at 170 s. The electric heating test sample and the associated infrared thermal images for C/CNT-20% fiber are shown in Fig. 6d, which shows the heating process more clearly.

The humidity sensing measurements were carried out using C/CNT-20% fiber connected copper electrode as sensor module, as illustrated in Fig. 7a. The dependence of relative resistance changes ($\Delta R/R_0$) of C/CNT-20% fiber to humidity is demonstrated in Fig. 7b. Over the investigated relative humidity range between 30 and 100%, the value of $\Delta R/R_0$ increases monotonically as the humidity increases. In typical CNT composites for liquid sensing, the resistance change of the material can be attributed to (1) changes in carrier concentration due to adsorbed molecules on the surface of the CNTs, and (2) swelling of the polymer matrix, altering the electron transport between conducting CNT networks (Zhao et al. 2020; Qi et al. 2014). For the cellulose/CNT composite fibers, CNTs are tightly coated with cellulose microfibers, the swelling of the cellulose plays a major role in the water sensing mechanism of this fiber. When the water molecules enter or leave the amorphous region of cellulose, the molecular chains will move apart or draw closer together, which alters the electron transport by varying the inter-nanotube distance between neighbor CNTs above or below the tunneling distance, causing the unique reversibility of the composites' electrical resistance. Benefitting from this property, the C/CNT composite fibers can be used as humidity sensors. As shown in Fig. 7c, d, the C/CNT-20% fiber was placed 100 cm from the human mouth to monitor the signal of resistance change for 10 breath cycles. The value of $\Delta R/R_0$ increases and decreases rapidly corresponding to breath exhalation and inhalation, which is attributed to a reversible hygroscopic swelling of the cellulose matrix. Drastic resistance change could be observed when the C/CNT-20% specimen was immersed in water, which can be seen in Fig. 7e-f. While during the drying process via hot air, $\Delta R/R_0$ values return to their initial base level. It's worth noting that after 4 wetting–drying cycles, the resistance curve of the specimen exhibited excellent stability and reproducibility. Although systematic research is still needed to clarify the performance of C/CNT composite fibers, this fast and reversible water sensing property indicated a good application prospect in humidity sensing for these fibers, such as smart fabric for monitoring human sweat.

Conclusions

In summary, a series of cellulose/CNT composite fibers was fabricated via a simple wet spinning method using an aqueous NaOH/urea system as solvent. Benefiting from the strong interaction between cellulose and CNT, along with the directional arrangement of CNTs in fibers matrix, which make the prepared fibers, such as the C/CNT-20% sample, exhibit good mechanical and conductive properties, with the tensile strength of 185 ± 9 MPa and electrical conductivity value of 1274 S/m. This intrinsic conductivity combined with hygroscopic swelling of cellulose/CNT

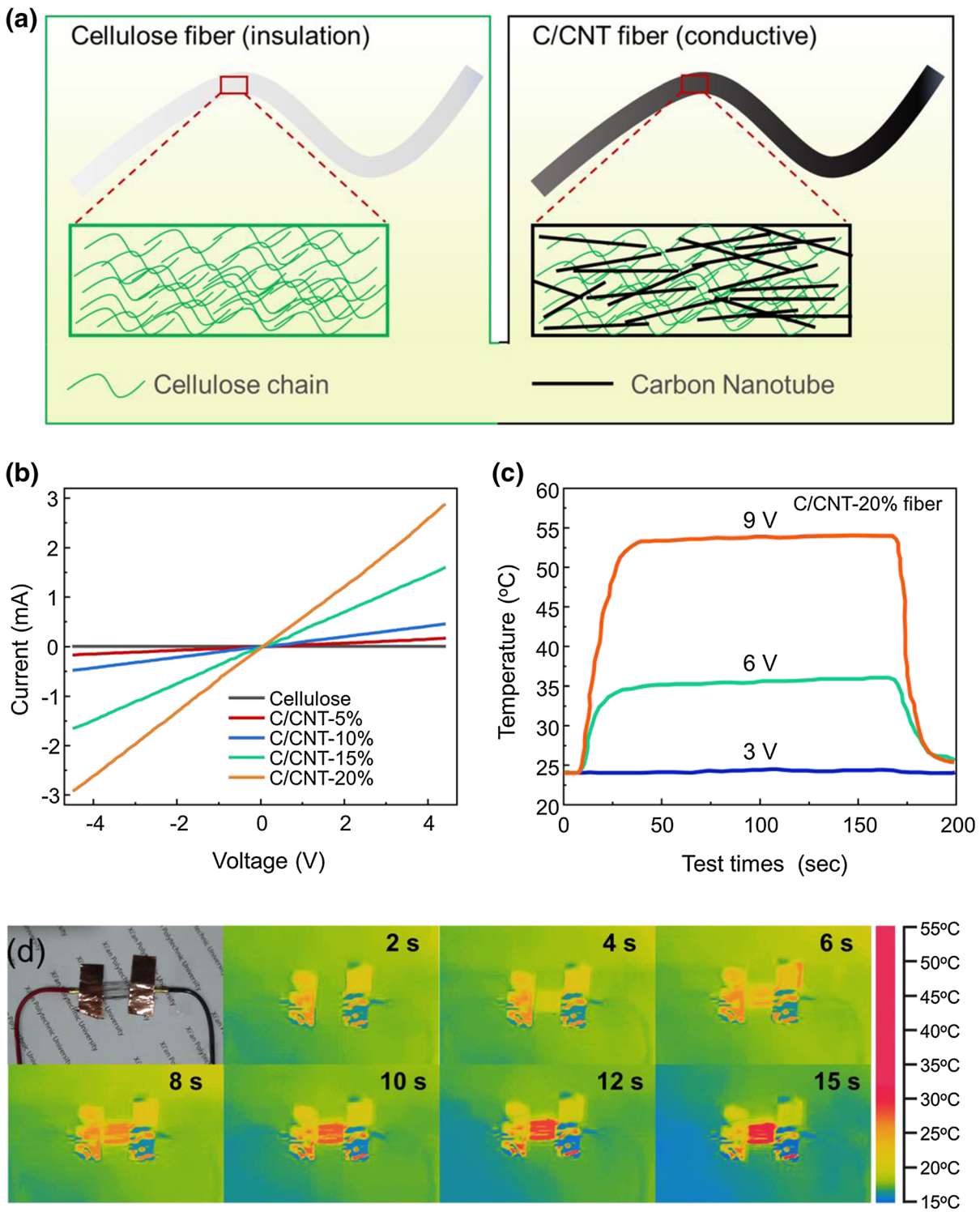

Fig. 6 **a** Schematic diagram of the conductive structure of cellulose/CNT composite fiber; **b** Current–voltage tests of C/CNT composite fiber with different CNT contents; **c** Time-dependent temperature changes of C/CNT-20% composite fiber under different applied voltage; **d** Infrared images for the electric heater made of C/CNT-20% composite fiber under 9 V for electric heating experiments

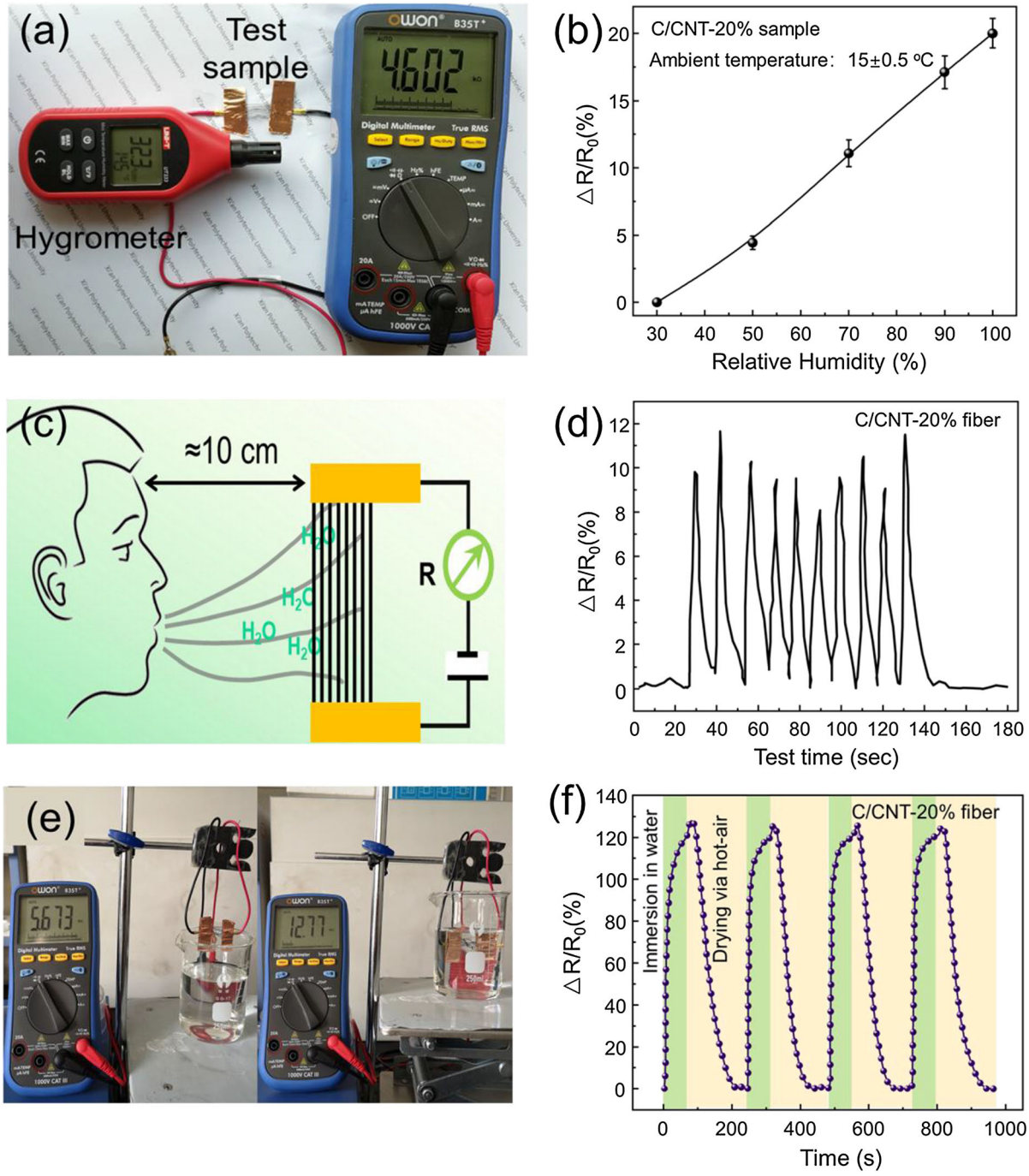

Fig. 7 **a** Humidity sensing test device with commercial hygrometers as reference; **b** Dependence of relative resistance change ($\Delta R/R_0$) on relative humidity; **c** Schematic for in-situ monitoring electrical resistance changes of the C/CNT-20% fiber placed at a distance about 100 mm from one's mouth; **d** Dependence of $\Delta R/R_0$ on test time for in-situ monitoring human breathing cycles; **e** Photograph of the liquid sensing test before and after being submerged in water; **f** $\Delta R/R_0$ of C/CNT-20% fiber sensor during successive wetting–drying cycles in water/air

composite fiber to make a material that can be used either as an electric heater or a humidity sensor. Through the Joule heating and humidity sensing measurements, we can conclude that the C/CNT-20% fiber exhibited an outstanding electric heating performance, as the heating temperature reaches more than 55 °C within 15 s at 9 V. In addition, this composite fiber showed an excellent humidity sensitivity at ambient temperature, no matter for humidity change caused by breathing or immersing in water. Combined with its scalable production process, flexible fiber morphology as well as multifunction feature, this cellulose/CNT composite fiber may open new opportunity for the development of lightweight and flexible fabrics in the field of wearable electronics and for the design of various smart flexible fabrics.

Acknowledgments This study was funded by National Natural Science Foundation of China (51903198), Scientific Research Program Funded by Shaanxi Provincial Education Department (20JY025), Innovation Capability Support Program of Shaanxi (2020TD-010), Open Research Project by State Key Laboratory of Polymer Molecular Engineering of Fudan University (K2020-25), Xi'an Polytechnic University-Shaoxing Keqiao West-Tex Textile Industry Innovative Institute Collaborative innovation project (19KQZD13).

Author contributions JM, CW and YW conceived the idea and designed the experiments. HP and PH carry out the experiment as well as the test characterization. QZ and SP discussed the results and commented on the manuscript. All the authors have approved the final version of the manuscript.

Declarations

Conflict of interest The authors declare that they have no known competing financial interest or personal relationships that could have appeared to influence the work reported in this paper.

Ethical approval All procedures performed in studies involving human participants were in accordance with the ethical standards of the institutional and/or national research committee and with the 1964 Helsinki declaration and its later amendments or comparable ethical standards.

Informed consent Informed consent was obtained from all individual participants included in the study.

References

Blanchard NP, Hatton RA, Silva SRP (2007) Tuning the work function of surface oxidised multi-wall carbon nanotubes via cation exchange. Chem Phys Lett 434(1–3):92–95. https://doi.org/10.1016/j.cplett.2006.11.100

Bober P, Liu J, Mikkonen KS, Ihalainen P, Pesonen M, Plumed-Ferrer C, Wright AV, Lindfors T, Xu CL, Latonen RM (2014) Biocomposites of nanofibrillated cellulose, polypyrrole, and silver nanoparticles with electroconductive and antimicrobial properties. Biomacromol 15(10):3655–3663. https://doi.org/10.1021/bm500939x

Cai J, Zhang LN, Chang CY, Cheng GZ, Chen XM, Chu B (2007) Hydrogen-bond-induced inclusion complex in aqueous cellulose/LiOH/urea solution at low temperature. ChemPhysChem 8(10):1572–1579. https://doi.org/10.1002/cphc.200700229

Cai J, Zhang L, Liu SL, Liu YT, Xu XJ, Chen XM, Chu B, Guo XL, Xu J, Cheng H, Han CC, Kuga S (2008) Dynamic self-assembly induced rapid dissolution of cellulose at low temperatures. Macromolecules 41(23):9345–9351. https://doi.org/10.1021/ma801110g

Carrasco PM, Montes S, Garcia I, Borghei M, Jiang H, Odriozola I, Cabanero G, Ruiz V (2014) High-concentration aqueous dispersions of graphene produced by exfoliation of graphite using cellulose nanocrystals. Carbon 70:157–163. https://doi.org/10.1016/j.carbon.2013.12.086

Chen Y, Potschke P, Pionteck J, Voit B, Qi HS (2018) Smart cellulose/graphene composites fabricated by in situ chemical reduction of graphene oxide for multiple sensing applications. J Mater Chem A 6(17):7777–7785. https://doi.org/10.1039/C8TA00618K

Cho SY, Yu H, Choi J, Kang H, Park S, Jang JS, Hong HJ, Kim ID, Lee SK, Jeong HS, Jung HT (2019) Continuous meter-scale synthesis of weavable tunicate cellulose/carbon nanotube fibers for high-performance wearable sensors. ACS Nano 13(8):9332–9341

Dichiara AB, Song A, Goodman SM, He D, Bai J (2017) Smart papers comprising carbon nanotubes and cellulose microfibers for multifunctional sensing applications. J Mater Chem A 5(38):20161–20169. https://doi.org/10.1039/C7TA04329E

Ferreira ES, Silva DS, Burgo TAL, Batista BC, Galembeck F (2017) Graphite exfoliation in cellulose solutions. Nanoscale 9(29):10219–10226. https://doi.org/10.1039/C7NR02365K

Hamedi MM, Hajian A, Fall AB, Hakansson K, Salajkova M, Lundell F, Wagberg L, Berglund LA (2014) Highly conducting, strong nanocomposites based on nanocellulose-assisted aqueous dispersions of single-wall carbon nanotubes. ACS Nano 8(3):2467–2476. https://doi.org/10.1021/nn4060368

Hardelin L, Hagstrom B (2015) Wet spun fibers from solutions of cellulose in an ionic liquid with suspended carbon nanoparticles. J Appl Polym Sci 132(6):41417. https://doi.org/10.1002/APP.41417

Huang HD, Liu CY, Zhang LQ, Zhong GJ, Li ZM (2015) Simultaneous reinforcement and toughening of carbon nanotube/cellulose conductive nanocomposite films by interfacial hydrogen bonding. ACS Sustain Chem Eng 3(2):317–324. https://doi.org/10.1021/sc500681v

Jiang ZM, Chen DN, Yu YQ, Miao JJ, Liu Y, Zhang LP (2017a) Composite fibers prepared from multi-walled carbon nanotubes/cellulose dispersed/dissolved in ammonium/

dimethyl sulfoxide mixed solvent. RSC Adv 7(4):2186–2192. https://doi.org/10.1039/C6RA25318K

Jiang ZW, Fang Y, Xiang JF, Ma YP, Lu A, Kang HL, Huang Y, Guo HX, Liu RG, Zhang LN (2014) Intermolecular interactions and 3D structure in cellulose-NaOH-urea aqueous system. J Phys Chem B 118(34):10250–10257. https://doi.org/10.1021/jp501408e

Jiang ZW, Fang Y, Ma YP, Liu M, Liu RG, Guo HX, Lu A, Zhang L (2017b) Dissolution and metastable solution of cellulose in NaOH/thiourea at 8°C for construction of nanofibers. J Phys Chem B 121(8):1793–1801. https://doi.org/10.1021/acs.jpcb.6b10829

Klemm D, Heublein B, Fink HP, Bohn A (2005) Cellulose: fascinating biopolymer and sustainable raw material. Angew Chem Int Edit 44(22):3358–3393. https://doi.org/10.1002/chin.200536238

Koga H, Saito T, Kitaoka T, Nogi M, Suganuma K, Isogai A (2013) Transparent, conductive, and printable composites consisting of TEMPO-oxidized nanocellulose and carbon nanotube. Biomacromol 14(4):1160–1165. https://doi.org/10.1021/bm400075f

Kontturi E, Laaksonen P, Linder MB, Nonappa GAH, Rojas OJ, Ikkala O (2018) Advanced materials through assembly of nanocelluloses. Adv Mater 30(24):1703779. https://doi.org/10.1002/adma.201703779

Lee TW, Han M, Lee SE, Jeong YG (2016a) Electrically conductive and strong cellulose-based composite fibers reinforced with multiwalled carbon nanotube containing multiple hydrogen bonding moiety. Compos Sci Technol 123:57–64. https://doi.org/10.1016/j.compscitech.2015.12.006

Lee TW, Lee SE, Jeong YG (2016b) Carbon nanotube/cellulose papers with high performance in electric heating and electromagnetic interference shielding. Compos Sci Technol 131:77–87. https://doi.org/10.1016/j.compscitech.2016.06.003

Li YY, Zhu HL, Wang YB, Ray U, Zhu SZ, Dai JQ, Chen CJ, Fu K, Jang SH, Henderson D, Li T, Hu LB (2017) Cellulose-nanofiber-enabled 3D printing of a carbon-nanotube microfiber network. Small Methods 1(10):1700222. https://doi.org/10.1002/smtd.201700222

Ma JH, Wang P, Dong L, Ruan YB, Lu HB (2019) Highly conductive, mechanically strong graphene monolith assembled by three-dimensional printing of large graphene oxide. J Colloid Interf Sci 534:12–19. https://doi.org/10.1016/j.jcis.2018.08.096

Mahmoudian S, Sazegar MR, Afshari N, Wahit MU (2017) Graphene reinforced regenerated cellulose nanocomposite fibers prepared by lyocell process. Polym Compos 38:81–88. https://doi.org/10.1002/pc.23864

Qi HS, Liu JW, Gao SL, Mader E (2013) Multifunctional films composed of carbon nanotubes and cellulose regenerated from alkaline-urea solution. J Mater Chem A 1(6):2161–2168. https://doi.org/10.1039/C2TA00882C

Qi H, Liu J, Deng Y, Gao S, Mäder E (2014) Cellulose fibres with carbon nanotube networks for water sensing. J Mater Chem A 2(15):5541–5547. https://doi.org/10.1039/C3TA14820C

Qi HS, Schulz B, Vad T, Liu JW, Mader E, Seide G, Gries T (2015) Novel carbon nanotube/cellulose composite fibers as multifunctional materials. ACS Appl Mater Inter 7(40):22404–22412. https://doi.org/10.1021/acsami.5b06229

Shi XW, Hu YL, Fu FY, Zhou JP, Wang YX, Chen LY, Zhang HM, Li J, Wang XH, Zhang LN (2014) Construction of PANI-cellulose composite fibers with good antistatic properties. J Mater Chem A 2(21):7669–7673. https://doi.org/10.1039/C4TA01149J

Siqueira G, Kokkinis D, Libanori R, Hausmann MK, Gladman AS, Neels A, Tingaut P, Zimmermann T, Lewis JA, Studart AR (2017) Cellulose nanocrystal inks for 3D printing of textured cellular architectures. Adv Funct Mater 27(12):1604619. https://doi.org/10.1002/adfm.201604619

Sun HB, Miao JJ, Yu YQ, Zhang LP (2015) Dissolution of cellulose with a novel solvent and formation of regenerated cellulose fiber. Appl Phys A-Mater 119(2):539–546. https://doi.org/10.1007/s00339-015-8986-6

Wan ZM, Chen CC, Meng TT, Mojtaba M, Teng YC, Feng Q, Li DG (2019) Multifunctional wet-spun filaments through robust nanocellulose networks wrapping to single-walled carbon nanotubes. ACS Appl Mater Inter 11(45):42808–42817. https://doi.org/10.1021/acsami.9b15153

Wang JF, Huang S, Lu X, Xu ZG, Zhao Y, Li JL, Wang XG (2017) Wet-spinning of highly conductive nanocellulose-silver fibers. J Mater Chem C 37(5):9673–9679. https://doi.org/10.1039/C7TC03217J

Wang QW, Zhang HB, Liu J, Zhao S, Xie X, Liu L, Yang R, Koratkar N, Yu ZZ (2019) Multifunctional and water-resistant MXene-decorated polyester textiles with outstanding electromagnetic interference shielding and joule heating performances. Adv Funct Mater 29(7):1806819. https://doi.org/10.1002/adfm.201806819

Wepasnick KA, Smith BA, Schrote KE, Wilson HK, Diegelmann SR, Fairbrother DH (2011) Surface and structural characterization of multi-walled carbon nanotubes following different oxidative treatments. Carbon 49(1):24–36. https://doi.org/10.1016/j.carbon.2010.08.034

Yan Z, Chen S, Wang H, Wang B, Jiang J (2008) Biosynthesis of bacterial cellulose/multi-walled carbon nanotubes in agitated culture. Carbohyd Polym 74(3):659–665. https://doi.org/10.1016/j.carbpol.2008.04.028

Ye DD, Lei XJ, Li T, Cheng QY, Chang CY, Hu LB, Zhang LN (2019) Ultrahigh tough, super clear, and highly anisotropic nanofiber-structured regenerated cellulose films. ACS Nano 13(4):4843–4853. https://doi.org/10.1021/acsnano.9b02081

Zhang HR, Sun XW, Heng ZG, Chen Y, Zou HW, Liang M (2018) Robust and flexible cellulose nanofiber/multiwalled carbon nanotube film for high-performance electromagnetic interference shielding. Ind Eng Chem Res 57(50):17152–17160. https://doi.org/10.1021/acs.iecr.8b04573

Zhang H, Wang ZG, Zhang ZN, Wu J, Zhang J, He HS (2007) Regenerated-cellulose/multiwalled-carbon-nanotube composite fibers with enhanced mechanical properties prepared with the ionic liquid 1-allyl-3-methylimidazolium chloride. Adv Mater 19(5):698–704. https://doi.org/10.1002/adma.200600442

Zhao X, Wang LY, Tang CY, Zha XJ, Liu Y, Su BH, Ke K, Bao RY, Yang MB, Yang W (2020) Smart Ti3C2Tx MXene fabric with fast humidity response and joule heating for

healthcare and medical therapy applications. ACS Nano 14(7):8793–8805. https://doi.org/10.1021/acsnano.0c03391

Zhu KK, Qiu CB, Lu A, Luo LB, Guo JH, Cong HJ, Chen F, Liu XY, Zhang X, Wang H, Cai J, Fu Q, Zhang LN (2018) Mechanically strong multifilament fibers spun from cellulose solution via inducing formation of nanofibers. ACS Sustain Chem Eng 6(4):5314–5321. https://doi.org/10.1021/acssuschemeng.8b00039